

## Lattice Boltzmann scheme with real numbered solid density for the simulation of flow in porous media

Orla Dardis and John McCloskey

*School of Environmental Studies, University of Ulster, Coleraine, Northern Ireland*

(Received 16 June 1997)

A modified lattice Boltzmann scheme for the simulation of flow in porous media is introduced, where momentum loss due to the presence of solid obstacles to flow is incorporated into the evolution equation. A real numbered parameter specified at each lattice node is related to the density of solid scatterers and represents the effect of porous medium solid structure on hydrodynamics. This scheme removes both the need for spatial and temporal averaging and the microscopic length scales associated with important classes of porous media. A numerical study demonstrates the adherence of the approach to the Navier-Stokes equation with an effective damping term. The potential use of the scheme to aid permeability predictions in realistic geological materials is discussed. [S1063-651X(98)08404-9]

PACS number(s): 47.55.Mh, 47.11.+j, 47.15.-x

The original lattice gas automaton (LGA) approximation to the Navier-Stokes equations [1] has undergone progressive improvements and refinements in recent years and is now well established as a viable model for fluid flow in porous media [2]. The theoretical background involving the convergence of the LGA and later lattice Boltzmann (LB) scheme to the Navier-Stokes equations, through derivation of the macrodynamical equations for the large scale and long term behavior of conserved quantities (fluid density and momentum), is well documented [3–5]. The LGA approach models a fluid as a system of identical discrete fluid particles, propagating along the links of a lattice from node to node, with interactions through collisions at lattice nodes such that mass and momentum are conserved. However, particle densities defined as Boolean variables make the microdynamics of the LGA intrinsically noisy, requiring statistical averaging in lattice subregions over long times to obtain meaningful results. These statistical fluctuations were eliminated with the development of the lattice Boltzmann model [6] which neglects correlations between particles and models the lattice gas using a Boltzmann equation where mean particle distribution functions replace the individual particles at lattice nodes. Both the LGA and LB schemes are restricted by the form of the microscopic collision rules. This limits the range of transport properties of the modeled fluid and led to further developments in which the LGA collision operator was linearized about its equilibrium distribution function to give a collision matrix [7]. Then, in the lattice Bhatnagar-Gross-Krook (BGK) scheme, a further simplification replaced the collision matrix with relaxation at a constant rate determined by a single transport parameter  $\omega$ , the eigenvalue of the LB collision matrix [8].

Despite numerous publications on the theoretical background and accuracy of the approach through comparisons with traditional finite-difference schemes [9,10], relatively few researchers have focused on flow in porous media [2,11–17]. This may be due in part to the need to use very simplified medium geometry so that direct comparisons with traditional finite-difference solutions may be made. In such

simulations, the porous medium is represented as a collection of solid obstacles to flow. Boolean variables assigned to each node of the simulation grid make the node a void part of the pore space and open to flow, or part of the rock matrix and closed to flow. At solid nodes, a “bounce-back” or no-slip boundary condition is imposed on any incident fluid particle, reflecting it back into its incoming direction. This no-slip condition is a first order approximation to the zero wall velocity condition [19] and significant errors can be introduced when the dimension of the void space is too small (relative to the particle mean free path) for hydrodynamic correlations to develop, thus placing limitations on the size of porous media which can be studied. It has been reported that any void space within the modeled medium needs to be at least twice the mean free path of the fluid particles in order to resolve the flow properly [2,18]. In a recent study of flow in porous media [17], the physical dimension of the modeled medium was 0.2 cm. For most practical applications the scale of interest is much larger but the computational requirements of a LB simulation using a larger scale porous structure would be too great. Therefore this Boolean definition of pore space, although allowing flexibility in the introduction of arbitrary microstructure, introduces a microscopic length scale to the medium, as rock structure only develops a discrete appearance when viewed under the microscope. This problem has been addressed recently in flow simulations [16] where the porous medium is represented by a *continuous* permeability distribution. These permeabilities were determined from LGA simulations of Darcy flow with a probabilistic no-slip boundary condition. A power-law relationship between the probability of occurrence of a solid (medium) node and the measured permeability allowed a permeability distribution to be defined for use with the LGA. This eliminated the explicit Boolean representation of medium structure and its association with a characteristic microscopic scale. However, the scheme still suffered from the statistical fluctuations of the LGA. The reasoning behind the modified scheme outlined in the following sections, namely, the elimination of the microscopic Boolean porous structure, is in a similar spirit to [16].

However, the proposed modification makes use of the LB approach, thus avoiding the noisy hydrodynamics associated with the LGA, and incorporates the porous medium interaction term directly into the evolution equation. We begin with a brief outline of the LB scheme, followed by a description of its modification and then compare the results obtained with relationships found for a LGA study using Boolean solid scatterers.

Six moving particle distributions  $N_i$   $\{i=1,\dots,6\}$ , and one rest particle distribution,  $N_i$   $\{i=0\}$  reside at the nodes of a two-dimensional (2D) hexagonal lattice. The rest particle population contributes to the fluid density but not to momentum. Particle distributions are assigned unit velocities  $\mathbf{e}_i$  in one of the six lattice directions  $i$  where

$$\mathbf{e}_i = \left[ \cos \frac{2\pi(i-1)}{6}, \sin \frac{2\pi(i-1)}{6} \right], \quad i = 1, \dots, 6 \quad (1)$$

and the local fluid density  $\rho$  and velocity  $\mathbf{u}$  at each node are given by

$$\begin{aligned} \rho &= \sum_{i=0}^6 N_i, \\ \rho \mathbf{u} &= \sum_{i=1}^6 N_i \mathbf{e}_i. \end{aligned} \quad (2)$$

The lattice BGK scheme [8] based on the original Frisch-Hasslacher-Pomeau model [4] is implemented using an evolution equation for the propagation and interaction of the fluid particle populations on the lattice. The fluid particle density  $N_i$ , moving in direction  $i$ , at node  $x$  and time  $t + \Delta t$  is given by

$$N_i(\mathbf{x}, t + \Delta t) = N_i(\mathbf{x} - \mathbf{e}_i, t) + \Delta N_i^{\text{BGK}}(\mathbf{x} - \mathbf{e}_i, t), \quad (3)$$

where

$$\Delta N_i^{\text{BGK}}(\mathbf{x} - \mathbf{e}_i, t) = \omega [N_i^{\text{eq}}(\mathbf{x} - \mathbf{e}_i, t) - N_i(\mathbf{x} - \mathbf{e}_i, t)]. \quad (4)$$

Equation (4) accounts for particle collisions (the transfer of momentum) through relaxation to equilibrium at a rate determined by the relaxation parameter  $\omega$ . The relaxation parameter controls the viscosity of the fluid through  $\nu = 1/8[(2/\omega) - 1]$ . The equilibrium populations  $N_i^{\text{eq}}$  are given by

$$\begin{aligned} N_i^{\text{eq}}(\mathbf{x}, t) &= \rho(\mathbf{x}, t) \left[ \frac{1}{7} + \frac{1}{3}(\mathbf{e}_i \cdot \mathbf{u}) + \frac{2}{3}(\mathbf{e}_i \cdot \mathbf{u})(\mathbf{e}_i \cdot \mathbf{u}) - \frac{1}{6}(\mathbf{u} \cdot \mathbf{u}) \right], \\ N_0^{\text{eq}}(\mathbf{x}, t) &= \rho(\mathbf{x}, t) \left[ \frac{1}{7} - (\mathbf{u} \cdot \mathbf{u}) \right] \end{aligned} \quad (5)$$

and are specifically constructed to recover the Navier-Stokes equations in the low Mach number limit [8].

The porous medium no-slip boundary condition is incorporated into Eq. (3) using the following LB scheme:

$$\begin{aligned} N_i(\mathbf{x}, t + \Delta t) &= N_i(\mathbf{x} - \mathbf{e}_i, t) + \Delta N_i^{\text{PM}}(\mathbf{x}, t) + \Delta N_i^{\text{BGK}}(\mathbf{x} - \mathbf{e}_i, t), \\ \Delta N_i^{\text{PM}}(\mathbf{x}, t) &= n_s(\mathbf{x}) [N_{i+3}(\mathbf{x}, t) - N_i(\mathbf{x} - \mathbf{e}_i, t)]. \end{aligned} \quad (6)$$

The addition of  $\Delta N_i^{\text{PM}}$  accounts for the effect of the porous medium (PM) on the fluid and determines the redistribution

of particle momentum. The parameter which controls this partitioning of fluid momentum is the continuous variable  $n_s(x)$ , defined as the solid scatterer density per lattice node  $x$  where  $0 < n_s(x) < 1$ . For example, 100 solid scatterers on a lattice of dimension  $100 \times 100$  would result in an average scatterer density per node of 0.01 in the LGA, while the same situation is represented here by a uniform distribution of  $n_s(x) = 0.01$ . When  $n_s(x) = 0$ ,  $\Delta N_i^{\text{PM}} = 0$  and Eq. (6) reduces to Eq. (3) for a free fluid in a void medium. For the opposite case where a node is given the value of  $n_s(x) = 1$ , the no-slip condition applies and the node is rendered impermeable.

Since there are no analytical solutions for fluid flow in arbitrary porous medium structure, the scheme is tested with reference to relationships derived for a LGA study of flow where the porous medium is represented by a random distribution of solid scatterers [11]. To simulate Poiseuille flow, the boundary conditions, periodic in  $x$  and no slip in  $y$  [20] are imposed on a  $128^2$  lattice. The flow is driven by a body force to add momentum in the positive  $x$  direction. The analytical solution to the usual Navier-Stokes equation for these boundary conditions is the equation for a parabola centered around the axis of the channel. From [11], the addition of fixed solid scatterers reduces the fluid velocity, modifying the usual Navier-Stokes equation through the introduction of a velocity dependent damping term  $\alpha$ ,

$$\nu \frac{d^2 u}{dy^2} - \alpha u = \frac{1}{\rho} \frac{dp}{dx}. \quad (7)$$

The solution to Eq. (7) is

$$u(y) = -\frac{1}{\alpha} \frac{1}{\rho} \frac{dp}{dx} \left[ 1 - \frac{\cosh[r(y-H/2)]}{\cosh(rH/2)} \right], \quad (8)$$

where the coefficients  $\alpha$  and  $r$  are related through

$$r = \sqrt{\alpha/\nu} \quad (9)$$

and the no-slip condition is applied at the channel walls,  $u(0) = 0$  and  $u(H) = 0$ ,  $dp/dx$  is the applied pressure gradient,  $\nu = \eta/\rho$  is the kinematic viscosity of the fluid, and  $r$  and  $\alpha$  are parameters relating to  $n_s(x)$ . By considering the microscopic particle-scatterer interactions of the LGA and using the Boltzmann approximation which relies on low scatterer densities, a relationship between  $\alpha$  and  $n_s$  was derived [11],

$$\alpha = 2n_s. \quad (10)$$

Darcy's law was then modified to

$$u_x = \frac{1}{\rho \alpha} \frac{dp}{dx} \quad (11)$$

thus relating the permeability  $k$  of the medium to the damping term  $\alpha$  through

$$k = \frac{\eta}{\rho \alpha} = \frac{\nu}{\alpha} = \frac{\nu}{2n_s}. \quad (12)$$

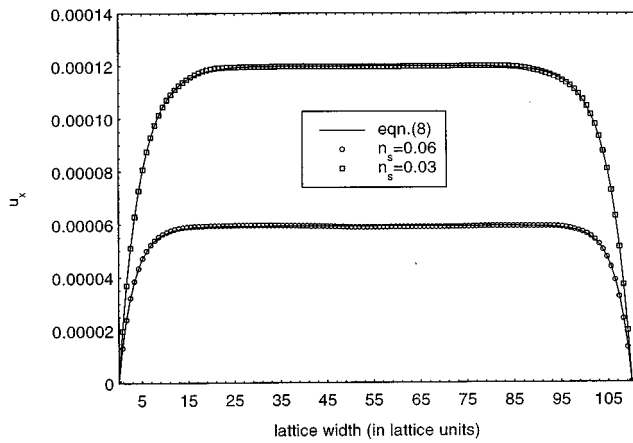


FIG. 1. Modified velocity profiles for different homogeneous distributions of  $n_s(x)$  with the corresponding fit to Eq. (8). The introduction of a nonzero  $n_s(x)$  lowers the average flow velocity. As  $n_s(x)$  is increased, the curvature of the profile decreases, leading to an increase in the measured damping term  $\alpha$  from [11].

Figure 1 shows two examples of the measured fluid velocity profiles for different homogeneous distributions of  $n_s(x)$ . The effective resistance to flow is quantified by obtaining  $\alpha$  and  $r$  from Eq. (8). This procedure requires no statistical averaging and is repeated for each uniform distribution of  $n_s(x) < 0.02$ . In Fig. 2, the parameters  $\alpha$  and  $r$ , obtained from velocity profiles similar to Fig. 1, allowed extraction of the viscosity  $\nu$  using Eq. (9). The measured value of 0.127 compares well with the analytical prediction of  $\nu = 0.125$  for  $\omega = 1.0$  from the BGK approximation. The relationship between  $\alpha$  and  $n_s$  is illustrated in Fig. 3 where  $\alpha = 2.04n_s$  in good agreement with Eq. (10). Finally, for different values of the applied body force, flow rates through the media were measured and permeabilities calculated from Darcy's law (11). Figure 4 shows the relationship between lattice permeability  $k$  and  $n_s(x)$  from Eq. (12). The best fit to the curve gives a kinematic viscosity of  $\nu = 0.1265$ . The relationships between  $k$ ,  $\alpha$ , and  $r$  derived in [11] for Darcy's law in the presence of scatterers hold, implying that the model intro-

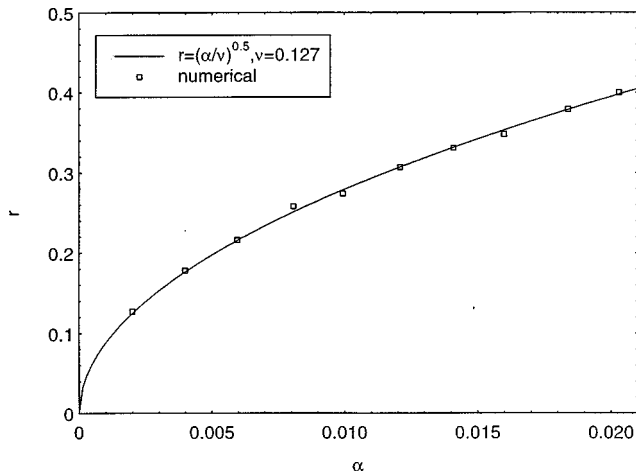


FIG. 2. Estimation of the fluid viscosity using Eq. (9). The measured viscosity of 0.127 is in good agreement with the theoretical value of 0.125.

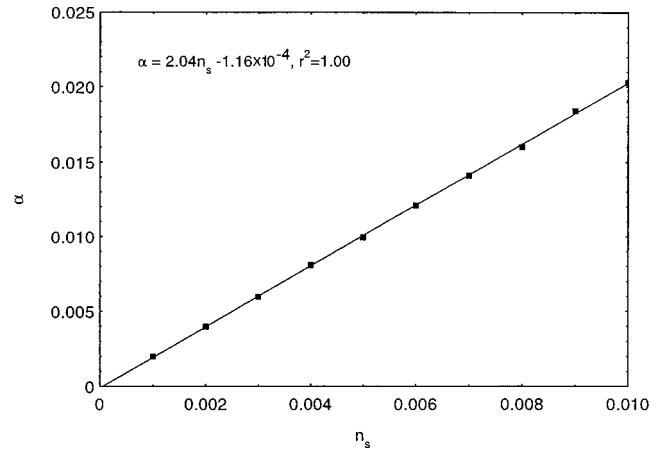


FIG. 3. Measured relationship between damping parameter  $\alpha$  and scatterer density  $n_s(x)$ . The result of  $\alpha = 2.04n_s$  compares well with Eq. (10).

duced here behaves in a similar fashion to an equivalent LGA scheme defined with a Boolean distribution of solid scatterers. The results are expected to hold for extension of the model to three dimensions, with the additional memory requirement of a real number  $n_s(x)$  at each lattice node in place of the Boolean variable used in previous 3D flow simulations [12].

The range of  $n_s(x)$  investigated in this study has been limited to values corresponding to a dilute system for comparative purposes and therefore the results presented are only valid for highly porous media. The range of porosity values for consolidated rock structure is considerably lower and the behavior of the model at high solid density has also been investigated [23], where permeability scaling laws consistent with percolation theory and experiment have been obtained. The advantage of applying a model using Eq. (6) to the problem of flow in porous media can be explained by visualizing the porous medium as a continuous space dependent distribution of  $n_s(x)$  rather than modeling detailed medium structure at a scale below the limit of meaningful laboratory and field studies. The elimination of Boolean porous structure allows the effect of correlated and anisotropic transport property distributions to be investigated by rastering the desired

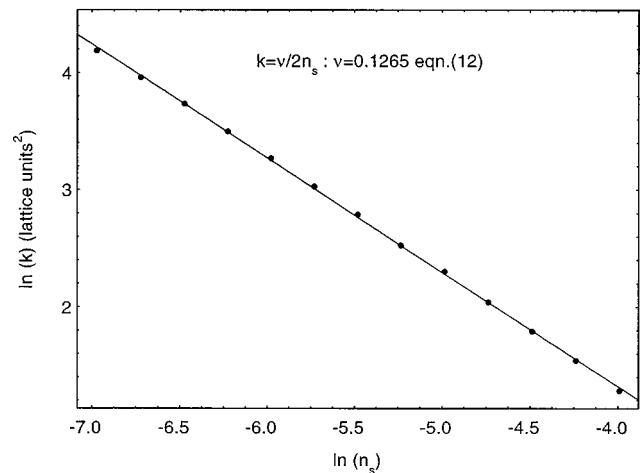


FIG. 4. The relationship between lattice permeability  $k$  and  $n_s(x)$  from Eq. (12) for homogeneous distributions of  $n_s(x)$ .

statistical distribution of  $n_s(x)$  onto the lattice. The dependence of transport properties in porous media on the size of the medium [21] and the determination of effective or equivalent transport parameters through upscaling is an important issue in groundwater hydrology and the petroleum

industry [22]. Work using the scheme to investigate the hydrodynamic behavior of correlated and anisotropic property fields and the dependence on system size and grid resolution (through simulations performed on variable grid sizes and using different rescaling methods) is near completion.

- 
- [1] U. Frisch, B. Hasslacher, and Y. Pomeau, *Phys. Rev. Lett.* **56**, 1505 (1986).
- [2] D. Rothman, *Geophysics* **53**, 509 (1988).
- [3] S. Wolfram, *J. Stat. Phys.* **45**, 471 (1986).
- [4] U. Frisch *et al.*, *Complex Syst.* **1**, 649 (1987).
- [5] R. Benzi, S. Succi, and M. Vergassola, *Phys. Rep.* **222**, 145 (1992).
- [6] G. McNamara and G. Zanetti, *Phys. Rev. Lett.* **61**, 2332 (1988).
- [7] F. Higuera, S. Succi, and R. Benzi, *Europhys. Lett.* **9**, 663 (1989).
- [8] Y. Qian, D. d'Humieres, and P. Lallemand, *Europhys. Lett.* **17**, 479 (1992).
- [9] D. Noble, J. Georgiadis, and R. Buckius, *Int. J. Numer. Methods Fluids* **23**, 1 (1996).
- [10] M. Reider and J. Sterling, *Comput. Fluids* **24**, 459 (1995).
- [11] K. Balasubramanian, F. Hayot, and W. Saam, *Phys. Rev. A* **36**, 2248 (1987).
- [12] A. Cancelliere *et al.*, *Phys. Fluids A* **2**, 2085 (1990).
- [13] S. Succi, R. Benzi, and F. Higuera, *Physica D* **47**, 219 (1991).
- [14] S. Chen *et al.*, *Physica D* **47**, 72 (1991).
- [15] G. Kohring, *J. Stat. Phys.* **63**, 411 (1991).
- [16] Y. Gao and M. Sharma, *Transp. Porous Media* **17**, 1 (1994).
- [17] B. F erreol and D. Rothman, *Transp. Porous Media* **20**, 3 (1995).
- [18] G. Kohring, *J. Phys. II* **1**, 593 (1991).
- [19] S. Chen, D. Martinez, and R. Mei, *Phys. Fluids* **8**, 2527 (1996).
- [20] P. Ziegler, *J. Stat. Phys.* **71**, 1171 (1993).
- [21] S. Neuman, *Geophys. Res. Lett.* **21**, 349 (1994).
- [22] X. H. Wen and J. J. G omez-Hern andez, *Hydrology* **183**, ix (1996).
- [23] O. Dardis and J. McCloskey (unpublished).